The *sek-1* p38 MAP kinase pathway regulates Gq signaling in *C. elegans*

Jill M. Hoyt, Samuel K. Wilson, Madhuri Kasa, Jeremy S. Rise,

Irini Topalidou, Michael Ailion

Department of Biochemistry, University of Washington, Seattle, WA, 98195

Running Title: *sek-1* regulates Gq signaling

key words: p38 MAPK pathway, Gq signaling, animal behavior, *C. elegans*

Corresponding author:
Michael Ailion
Department of Biochemistry
University of Washington
Box 357350
1705 NE Pacific St
Seattle, WA 98195
Phone: 206-685-0111
email: mailion@uw.edu

Abstract

Gq is a heterotrimeric G protein that is widely expressed in neurons and regulates neuronal activity. To identify pathways regulating neuronal Gq signaling we performed a forward genetic screen in *Caenorhabditis elegans* for suppressors of activated Gq. One of the suppressors is an allele of *sek-1*, which encodes a mitogen-activated protein kinase kinase (MAPKK) in the p38 MAPK pathway. Here we show that *sek-1* mutants have a slow locomotion rate and that *sek-1* acts in acetylcholine neurons to regulate both locomotion and Gq signaling. Furthermore, we find that *sek-1* acts in mature neurons to regulate locomotion. Using genetic and behavioral approaches we demonstrate that other components of the p38 MAPK pathway also play a positive role in regulating locomotion and Gq signaling. Finally, we find that mutants in the *sek-1* p38 MAPK pathway partially suppress an activated mutant of the sodium leak channel NCA-1/NALCN, a downstream target of Gq signaling. Our results suggest that the *sek-1* p38 pathway may modulate the output of Gq signaling through NCA-1.

Introduction

Gq is a widely expressed heterotrimeric G protein that regulates a variety of biological processes ranging from neurotransmission to cardiovascular pathophysiology (Sánchez-Fernández et al., 2014). In the canonical Gq pathway, Gq activates phospholipase Cβ (PLCβ), which cleaves phosphatidylinositol 4,5-bisphosphate (PIP_2) into the second messengers diacylglycerol (DAG) and inositol trisphosphate (IP_3) (Rhee, 2001). In addition to PLCβ, other Gq effectors have been identified including kinases, such as protein kinase Cζ (PKCζ) and Bruton's tyrosine kinase (Btk) (Bence et al., 1997; García-Hoz et al., 2010), and guanine nucleotide exchange factors (GEFs) for the small GTPase Rho, such as Trio (Williams et al., 2007; Vaqué et al., 2013). These noncanonical effectors bridge the activation of Gq to other cellular signaling cascades.

In order to study noncanonical pathways downstream of Gq, we used the nematode *C. elegans* which has a single Gαq homolog (EGL-30) and conservation of the other components of the Gq signaling pathway (Koelle, 2016). In neurons, EGL-30 signals through EGL-8 (PLCβ) (Lackner et al., 1999) and UNC-73 (ortholog of Trio RhoGEF) (Williams et al., 2007). UNC-73 activates RHO-1 (ortholog of RhoA), which has been shown to enhance neurotransmitter release through both diacylglycerol kinase (DGK-1)-dependent and DGK-1-independent pathways (McMullan et al., 2006).

To identify additional signaling pathways that modulate Gq signaling, we screened for suppressors of the activated Gq mutant *egl-30(tg26)* (Doi and Iwasaki, 2002), hereafter referred to as *egl-30(gf). egl-30(gf)* mutant animals exhibit hyperactive locomotion and a "loopy" posture in which worms have exaggerated, deep body bends and loop onto themselves (Bastiani et al., 2003). Here we identify one of the

62 suppressors as a deletion allele in the gene *sek-1*. SEK-1 is a mitogen-activated protein
63 kinase kinase (MAPKK), the *C. elegans* ortholog of mammalian MKK3/6 in the p38
64 MAPK pathway (Tanaka-Hino et al., 2002). The p38 MAPK pathway has been best
65 characterized as a pathway activated by a variety of cellular stresses and inflammatory
66 cytokines (Kyriakis and Avruch, 2012). However, the p38 MAPK pathway has also been
67 shown to be activated downstream of a G protein-coupled receptor in rat neurons
68 (Huang et al., 2004). Btk, a member of the Tec family of tyrosine kinases, has been
69 shown to act downstream of Gq to activate the p38 MAPK pathway (Bence et al., 1997),
70 but *C. elegans* lacks Btk and other Tec family members (Plowman et al., 1999).
71 SEK-1 is activated by the MAPKKK NSY-1 (ortholog of ASK1) and activates the p38
72 MAPKs PMK-1 and PMK-2 (Andrusiak and Jin, 2016). The p38 MAPK pathway
73 consisting of NSY-1/SEK-1/PMK-1 is required for innate immunity in *C. elegans* (Kim et
74 al., 2002). NSY-1 and SEK-1 are also required for the specification of the asymmetric
75 AWC olfactory neurons (Sagasti et al., 2001; Tanaka-Hino et al., 2002); the p38
76 orthologs PMK-1 and PMK-2 function redundantly in AWC specification (Pagano et al.,
77 2015). For both innate immunity and AWC specification, the p38 MAPK pathway acts
78 downstream of the adaptor protein TIR-1 (an ortholog of SARM) (Couillault et al., 2004;
79 Chuang and Bargmann, 2005). Here we show that the TIR-1/NSY-1/SEK-1/PMK-1
80 PMK-2 signaling module also acts to regulate locomotion downstream of Gq signaling.
81

82 **Materials and Methods**

83 ***C. elegans strains and maintenance***

All strains were cultured using standard methods and maintained at 20°C (Brenner, 1974). The *sek-1(yak42)* mutant was isolated from an ENU mutagenesis suppressor screen of the activated Gq mutant *egl-30(tg26)* ("*egl-30(gf)*") (Ailion et al., 2014). *sek-1(yak42)* was outcrossed away from *egl-30(gf)* before further analysis. Double mutant strains were constructed using standard methods (Fay, 2006) often with linked fluorescent markers (Frokjaer-Jensen et al., 2014) to balance mutations with subtle visible phenotypes. Table S1 contains all the strains used in this study.

Mapping

yak42 was mapped using the slow locomotion phenotype and its *egl-30(gf)* suppression phenotype. *yak42* was initially mapped to Chromosome X using strains EG1000 and EG1020, which carry visible marker mutations. These experiments showed that *yak42* was linked to *lon-2*, but at least several map units away. *yak42* was further mapped to about one map unit (m.u.) away from the red fluorescent insertion marker *oxTi668* which is located at +0.19 m.u. on Chromosome X.

Whole-genome sequencing

Strain XZ1233 *egl-30(tg26); yak42* was used for whole-genome sequencing to identify candidate *yak42* mutations. XZ1233 was constructed by crossing a 2X outcrossed *yak42* strain back to *egl-30(tg26)*. Thus, in XZ1233, *yak42* has been outcrossed 3X from its original isolate. DNA was isolated from XZ1233 and purified according to the Hobert Lab protocol (http://hobertlab.org/whole-genome-sequencing/). Ion Torrent sequencing was performed at the University of Utah DNA Sequencing Core

Facility. The resulting data contained 10,063,209 reads of a mean read length of 144 bases, resulting in about 14X average coverage of the *C. elegans* genome. The sequencing data were uploaded to the CloudMap pipeline on the Galaxy platform (Minevich et al., 2012) and SNPs and indels were identified. We filtered out polymorphisms found in other strains we sequenced, leaving us with 605 homozygous mutations. Chromosome X contained 94 mutations: 55 SNPs and 39 indels. Of these, four SNPs were non-synonymous mutations in protein-coding genes, but only 2 were within 5 m.u. of *oxTi668.* However, we were unable to identify *yak42* from the candidate polymorphisms located near *oxTi668*. Transgenic expression of the most promising candidate *pcyt-1* (located at -1.49 m.u.) did not rescue *yak42*. Instead, to identify possible deletions, we scrolled through 2 MB of aligned reads on the UCSC Genome Browser starting at -4.38 m.u. and working towards the middle of the chromosome (0 m.u.), looking for regions that lacked sequence coverage. We found a 3713 bp deletion that was subsequently confirmed to be the *yak42* causal mutation, affecting the gene *sek-1* located at -1.14 m.u.

Locomotion assays

Locomotion assay plates were made by seeding 10 cm nematode growth medium plates with 150 µl of an OP50 (a strain of *E. coli*) stock culture, spread with sterile glass beads to cover the entire plate. Bacterial lawns were grown at room temperature (22.5°C -24.5°C) for 24 hrs and then stored at 4°C until needed. All locomotion assays were performed on first day adults. L4 stage larvae were picked the day before the assay and the experimenter was blind to the genotypes of the strains

assayed. For experiments on strains carrying extrachromosomal arrays, the *sek-1(km4)* control worms were animals that had lost the array from the same plate.

Body bends assays were performed as described (Miller et al., 1999). The locomotion assay plate was brought to room temperature (22.5°C -24.5°C). All strains in an experiment were assayed on the same assay plate. A single animal was picked onto the plate, the plate lid was returned, and the animal recovered for 30 s. Body bends were then counted for one minute. A body bend was counted each time the worm's tail reached the minimum or maximum amplitude of the sine wave. For experiments with *egl-8*, *unc-73*, and *rund-1*, worms were allowed a minimal recovery period (until the worms started moving forward, 5 sec maximum) prior to counting body bends.

For the heat shock experiment, plates of first-day adults were parafilmed and heatshocked in a 34°C water bath for 1 hr. Plates were then un-parafilmed and incubated at 20°C for five hours before performing body bend assays.

Radial locomotion assays were performed by first bringing the locomotion assay plates to room temperature. Animals were picked to the middle of the plate, the plate taped shut, and an x was marked on the lid above where the animals were placed. Assay plates were then incubated at 20°C for 20 hr and the distances of the worms from the starting point were measured.

Quantitative analysis of the waveform of worm tracks was performed by first bringing the locomotion assay plate to room temperature. One strain at a time, five animals were placed on the plate and allowed to roam for 2-5 min. We then took five pictures of each animal's tracks following forward locomotion. Track pictures were taken at 40X on a Nikon SMZ18 microscope with the DS-L3 camera control system. This

153 process was repeated for all strains per experiment set. Worm track pictures were
154 processed using ImageJ. Tracks were straightened with the segmented line tool and
155 pictures converted to grayscale. Period and 2X amplitude were measured freehand
156 using the line tool. For each worm, five period/amplitude ratios were calculated from
157 each of the five straightened tracks. The ratios were averaged for each worm and these
158 averages were averaged for each strain.
159
160 ***C. elegans pictures***
161 Pictures of worms were taken at 60X on a Nikon SMZ18 microscope with the DS-
162 L3 camera control system. The worms were age-matched as first day adults and each
163 experiment set was photographed on the same locomotion assay plate (assay plate
164 preparation described above). The images were processed using ImageJ and were
165 rotated, cropped, and converted to grayscale.
166
167 ***Molecular biology***
168 Plasmids were constructed using the Gateway cloning system (Invitrogen).
169 Plasmids and primers used are found in Table S2. The *sek-1* cDNA was amplified by
170 RT-PCR from worm RNA and cloned into a Gateway entry vector. To check for proper
171 expression of *sek-1*, an operon GFP was included in expression constructs with the
172 following template: (promoter)p::*sek-1*(cDNA)::*tbb-2utr::gpd-2 operon::GFP::H2B:cye-*
173 *1utr* (Frøkjær-Jensen et al., 2012). This resulted in untagged SEK-1, but expression
174 could be monitored by GFP expression.
175

176 ***Injections***

177 *C. elegans* strains with extrachromosomal arrays were generated by standard
178 methods (Mello et al., 1991). Injection mixes were made with a final total concentration
179 of 100 ng/µL DNA. Constructs were injected at 5 ng/µL, injection markers at 5 ng/µL,
180 and the carrier DNA Litmus 38i at 90 ng/µL. Multiple lines of animals carrying
181 extrachromosomal arrays were isolated and had similar behaviors as observed by eye.
182 The line with the highest transmittance of the array was assayed.

183

184 ***Statistical analysis***

185 At the beginning of the project, a power study was conducted on pilot body bend
186 assays using wild type and *sek-1(yak42)* worms. To achieve a power of 0.95, it was
187 calculated that 17 animals should be assayed per experiment. Data were analyzed to
188 check if normally distributed (using the D'Agostino-Pearson and Shapiro-Wilk normality
189 tests) and then subjected to the appropriate analysis using GraphPad Prism 5. For data
190 sets with three or more groups, if the data were normal they were analyzed with a one-
191 way ANOVA; if not, with a Kruskal-Wallis test. Post-hoc tests were used to compare
192 appropriate data sets within an experiment. Reported p-values are corrected. Table S3
193 contains the statistical tests for each experiment. $p<0.05$ = *; $p<0.01$ = **; $p<0.001$ = ***.

194

195 ***Reagent and Data Availability***

196 Strains and plasmids are shown in Table S1 and Table S2 and are available from
197 the *Caenorhabditis* Genetics Center (CGC) or upon request. The authors state that all

198 data necessary for confirming the conclusions presented in the article are represented
199 fully within the article and Supplemental Material.
200
201 **Results**
202 ***sek-1* suppresses activated Gq**
203 To identify downstream effectors of Gαq, we performed a forward genetic screen
204 for suppressors of the activated Gq mutant, *egl-30(tg26)* (Doi and Iwasaki, 2002),
205 referred to here as *egl-30(gf). egl-30(gf)* worms are small, hyperactive, and have a
206 "loopy" posture characterized by a high-amplitude waveform (Figure 1B). Thus, we
207 screened for worms that are larger, less hyperactive, and less loopy. We isolated a
208 recessive suppressor, *yak42*, and mapped it to the middle of Chromosome X (see
209 Materials and Methods). Whole-genome sequencing revealed that *yak42* carries a large
210 deletion of the *sek-1* gene from upstream of the start codon to exon 4 (Figure 1A).
211 *yak42* also failed to complement *sek-1(km4)*, a previously published *sek-1* deletion
212 allele (Figure 1A) (Tanaka-Hino et al., 2002).
213 *egl-30(gf)* double mutants with either *sek-1(yak42)* or *sek-1(km4)* are bigger than
214 *egl-30(gf)* worms (Figure 1B), not hyperactive (Figure 1C). and have a tendency to kink
215 when moving backward. Additionally, both *sek-1* mutations suppress the loopy
216 waveform phenotype (Figure S1A, B).
217 *sek-1(yak42)* was outcrossed from *egl-30(gf)* and assayed for locomotion
218 defects. Both the *sek-1(yak42)* and *sek-1(km4)* mutants are coordinated but move more
219 slowly than wild-type (Figure 1D). *sek-1(ag1)*, a point mutation in exon 5 (Kim et al.,
220 2002), also causes a similar slow locomotion phenotype (Figure S1C). To test whether

the *egl-30(gf)* suppression phenotype might be an indirect effect of the slow locomotion of a *sek-1* mutant, we built an *egl-30(gf)* double mutant with a mutation in *unc-82*, a gene required for normal muscle structure. *unc-82* mutants are coordinated but move slowly, similar to a *sek-1* mutant (Hoppe et al., 2010). However, although an *egl-30(gf) unc-82(e1220)* double mutant moves more slowly than *egl-30(gf)*, it is still small and loopy (Figure 1B). Thus, *sek-1* appears to be a specific suppressor of multiple phenotypes of the *egl-30(gf)* mutant, suggesting that *sek-1* regulates locomotion and acts downstream of Gq.

EGL-30/Gαq is negatively regulated by GOA-1, the worm Gαo/i ortholog (Hajdu-Cronin et al., 1999). We tested whether *sek-1* also suppresses a *goa-1* loss-of-function mutant that causes a hyperactive phenotype similar to *egl-30(gf).* Indeed, *sek-1(km4)* suppresses *goa-1(sa734)* (Figure S1D). One downstream effector of GOA-1 is the DAG kinase DGK-1 (DGKΘ ortholog) that inhibits DAG-dependent functions such as synaptic vesicle release (Nurrish *et al.* 1999; Miller *et al.* 1999). *dgk-1(sy428)* animals are hyperactive, but *sek-1(km4)* does not suppress *dgk-1*. Rather, the *sek-1 dgk-1* double mutant is uncoordinated and looks like neither *sek-1* nor *dgk-1* mutants, confounding the interpretation of how *sek-1* genetically interacts with *dgk-1*.

sek-1 acts in mature acetylcholine neurons

egl-30 is widely expressed and acts in neurons to regulate locomotion (Lackner et al., 1999), so it is possible that *sek-1* also acts in neurons to regulate Gq signaling. *sek-1* is expressed in neurons, intestine, and several other tissues (Tanaka-Hino et al.,

2002) and has been shown to function in GABA neurons to possibly promote GABA release (Vashlishan et al., 2008).

To identify the cell type responsible for the *sek-1* locomotion phenotypes, we expressed the wild-type *sek-1* cDNA under different cell-specific promoters and tested for transgenic rescue of a *sek-1* null mutant. Expression of *sek-1* in all neurons (using the *unc-119* promoter) or in acetylcholine neurons (using *unc-17p*) was sufficient to rescue the *sek-1* mutant slow locomotion phenotype, but expression in GABA neurons (using *unc-47p*) was not sufficient to rescue (Figure 2A, B). These results indicate that *sek-1* acts in acetylcholine neurons to regulate locomotion.

We next tested whether *sek-1* also acts in neurons to suppress *egl-30(gf)*. Expression of *sek-1* under pan-neuronal and acetylcholine neuron promoters rescued the *sek-1* suppression of *egl-30(gf)*. Specifically, *egl-30(gf) sek-1* double mutants expressing wild-type *sek-1* in all neurons or acetylcholine neurons had a hyperactive, loopy, small phenotype that resembled the *egl-30(gf)* single mutant (Figure 2C, D). However, expression of *sek-1* in GABA neurons did not rescue the suppression phenotype (Figure 2C, D). Together, these data show that *sek-1* acts in acetylcholine and not GABA neurons to regulate both wild-type locomotion and to modulate Gq signaling.

Because *sek-1* acts in the development of the AWC asymmetric neurons, we asked whether *sek-1* also has a developmental role in regulating locomotion by testing whether adult-specific *sek-1* expression (driven by a heat-shock promoter) is sufficient to rescue the *sek-1* mutant. We found that *sek-1* expression in adults rescues the *sek-1* slow locomotion phenotype (Figure 2E). This result indicates that *sek-1* is not required

for development of the locomotion circuit and instead acts in mature neurons to regulate locomotion.

The p38 MAPK pathway is a positive regulator of Gq signaling

SEK-1 is the MAPKK in a p38 MAPK pathway (Tanaka-Hino et al., 2002). This pathway consists of NSY-1 (MAPKKK), SEK-1 (MAPKK), and PMK-1 or PMK-2 (MAPKs)(Andrusiak and Jin, 2016). TIR-1 acts upstream of NSY-1. This p38 MAPK signaling module has been shown to function in innate immunity and the development of the AWC olfactory neurons (Chuang and Bargmann, 2005).

We tested whether the entire p38 MAPK and TIR-1 signaling module also regulates locomotion and suppression of activated Gq. Both *tir-1(tm3036)* and *nsy-1(ok593)* mutant animals have slow locomotion on their own and also suppress the hyperactivity, deep body bends and small size of *egl-30(gf)* (Figure 3A-D; Figure S2A, B). We also tested single mutants in each of the three worm p38 MAPK genes (*pmk-1, pmk-2* and *pmk-3)* and a *pmk-2 pmk-1* double mutant. Although we found that the *pmk-2* and *pmk-3* single mutants were slightly slow on their own, only the *pmk-2 pmk-1* double mutant phenocopied *sek-1* and suppressed both the hyperactivity and deep body bends of *egl-30(gf)* (Figure 3, E-G). Thus, *pmk-2* and *pmk-1* act redundantly downstream of *sek-1* to suppress *egl-30(gf).* These data suggest that the p38 MAPK pathway regulates locomotion in *C. elegans* and acts genetically downstream of *egl-30*.

The JNK MAPK pathway, related to the p38 MAPK family, also regulates locomotion in *C. elegans*. Specifically, the JNK pathway members *jkk-1* (JNK MAPKK) and *jnk-1* (JNK MAPK) have been shown to act in GABA neurons to regulate

289 locomotion (Kawasaki et al., 1999). We found that the *jkk-1* and *jnk-1* single mutants
290 had slow locomotion and that the double mutants with p38 MAPK pathway members
291 exhibited an additive slow locomotion phenotype (Figure S2C). Moreover, neither *jkk-1*
292 nor *jnk-1* suppressed *egl-30(gf)* (data not shown). Thus, the JNK and p38 MAPK
293 pathways regulate locomotion independently and the JNK pathway is not involved in Gq
294 signaling.

295 We also tested the involvement of possible p38 MAPK pathway effectors. One of
296 the targets of PMK-1 is the transcription factor ATF-7 (Shivers et al., 2010). Both the *atf-*
297 *7(qd22 qd130)* loss-of-function mutant and the *atf-7(qd22)* gain-of-function mutant
298 moved slowly compared to wild-type animals (Figure S2D). However, *atf-7(qd22 qd130)*
299 did not suppress *egl-30(gf)* (data not shown), suggesting that *atf-7* is not a target of this
300 pathway or acts redundantly with other downstream p38 MAPK targets. We also tested
301 *gap-2*, the closest *C. elegans* homolog of ASK1-interacting Protein (AIP1) which
302 activates ASK1 (the ortholog of *C. elegans* NSY-1) in mammalian systems (Zhang et
303 al., 2003). A *C. elegans gap-2* mutant has no locomotion defect (Figure S2E). Finally,
304 we tested VHP-1, a phosphatase for p38 and JNK MAPKs that inhibits p38 MAPK
305 signaling (Kim et al., 2004). However, the *vhp-1(sa366)* mutant also has no locomotion
306 defect (Figure S2E).

307 *egl-30(gf)* animals are loopy and hyperactive so we tested whether increased
308 activation of the TIR-1/p38 MAPK signaling module causes similar phenotypes. The *tir-*
309 *1(ky648gf)* allele leads to a gain-of-function phenotype in the AWC neuron specification
310 (Chang et al., 2011), but does not cause a locomotion phenotype reminiscent of *egl-*
311 *30(gf)* (Figure S2F, G).

312

313 **Genetic interactions of *sek-1* with pathways acting downstream of Gq**

314 Our forward genetic screen for suppressors of *egl-30(gf)* identified mutants that
315 fall into three different categories: mutants in the canonical Gq pathway such as the
316 PLC *egl-8* (Lackner et al., 1999), mutants in the RhoGEF Trio pathway such as *unc-73*
317 (Williams et al., 2007), and mutants that affect dense-core vesicle biogenesis and
318 release (Ailion et al., 2014; Topalidou et al., 2016a).

319 To test if *sek-1* acts in these pathways we used genetic epistasis analysis. Loss-
320 of-function alleles of *egl-8(sa47)*, *unc-73(ox317),* and *rund-1(tm3622)* have slow
321 locomotion (Figure 4A-C). Our data show that *sek-1* enhances the phenotype of *egl-8*
322 and *rund-1* single mutants, suggesting that *sek-1* does not act in the same pathway as
323 *egl-8* or *rund-1* (Figure 4A, B). By contrast, *sek-1* does not enhance the slow locomotion
324 phenotype of *unc-73* mutants (Figure 4C), suggesting that *sek-1* may act in the same
325 genetic pathway as the Trio RhoGEF *unc-73.*

326 We next tested whether *sek-1* interacts with *rho-1*, encoding the small G protein
327 activated by Trio. *rho-1* is required for viability so we could not use a loss-of-function
328 allele to test for a genetic interaction (Jantsch-Plunger et al., 2000). Instead we used an
329 integrated transgene overexpressing an activated *rho-1* mutant allele specifically in
330 acetylcholine neurons. Animals carrying this activated RHO-1 transgene, referred to
331 here as *rho-1(gf)*, have a loopy posture reminiscent of *egl-30(gf)* (McMullan et al.,
332 2006), and a decreased locomotion rate. *rho-1(gf) sek-1(km4)* double mutants had a
333 loopy body posture like *rho-1(gf)* and an even slower locomotion rate (Figure 4D, E),
334 suggesting that *sek-1* and *rho-1(gf)* mutants have additive locomotion phenotypes.

However, both *sek-1(km4)* and *sek-1(yak42)* suppress the slow growth rate of the *rho-1(gf)* mutant. Because *sek-1* does not enhance *unc-73* mutants and suppresses some aspects of the *rho-1(gf)* mutant, *sek-1* may modulate output of the Rho pathway, though it probably is not a direct transducer of Rho signaling.

sek-1 and _nsy-1_ partially suppress activated NCA

The data above did not clarify the relationship of *sek-1* to the Rho pathway acting downstream of Gq. The downstream target of this Gq-Rho pathway appears to be the NCA-1 cation channel (Topalidou et al., 2016b). NCA-1 and its orthologs are sodium leak channels associated with rhythmic behaviors in several organisms (Nash et al., 2002; Lu et al., 2007; Shi et al., 2016). In *C. elegans*, NCA-1 potentiates persistent motor circuit activity and sustains locomotion (Gao et al., 2015).

To examine interactions of the *sek-1* p38 MAPK pathway with NCA-1, we tested whether *sek-1* and *nsy-1* mutants suppress the activated NCA-1 mutant *ox352*, referred to as *nca-1(gf)*. The *nca-1(gf)* animals are coiled and uncoordinated; thus, it is difficult to measure their locomotion rate by the body bend assay because they sometimes do not propagate sinusoidal waves down the entire length of their body. Instead, we used a radial locomotion assay in which we placed animals in the center of a 10 cm plate and later measured how far the animals had moved. *nca-1(gf)* double mutants with either *sek-1(km4)* or *nsy-1(ok593)* uncoil a bit but still exhibit uncoordinated locomotion (Figure 5A). In fact, though these double mutants show more movement in the anterior half of their bodies than *nca-1(gf)*, they propagate body waves to their posterior half even more poorly than the *nca-1(gf)* mutant. However, both *sek-1* and *nsy-1* clearly

suppress the small size and slow growth rate of the *nca-1(gf)* mutant (Figure 5A) and in radial locomotion assays, *sek-1* and *nsy-1* weakly suppressed the *nca-1(gf)* locomotion phenotype (Figure 5B). Together these data suggest that mutants in the *sek-1* p38 MAPK pathway partially suppress some aspects of the *nca-1(gf)* mutant.

Given that *sek-1* acts in acetylcholine neurons to regulate wild-type and *egl-30(gf)* locomotion, we tested if the same neuron class is responsible for *sek-1* suppression of *nca-1(gf)*. Expression of *sek-1* in all neurons or in acetylcholine neurons of *nca-1(gf) sek-1(km4)* animals restored the *nca-1(gf)* size and posture phenotypes. These worms are small and coiled and closely resemble the *nca-1(gf)* mutant (Figure 5C). By contrast, expression of *sek-1* in GABA neurons did not affect the size or posture of the *nca-1(gf) sek-1* double mutant (Figure 5C). These data suggest that *sek-1* acts in acetylcholine neurons to regulate *nca-1(gf)* locomotion. However, in radial locomotion assays, expression of *sek-1* in none of these neuron classes significantly altered the movement of the *nca-1(gf) sek-1* double mutant (Figure 5D), though the weak suppression of *nca-1(gf)* by *sek-1* in this assay makes it difficult to interpret these negative results. We make the tentative conclusion that *sek-1* partially suppresses *nca-1(gf)* locomotion and probably acts in the acetylcholine neurons where it also acts to regulate wild-type and *egl-30(gf)* locomotion, suggesting a common neuronal site of action of this pathway.

Discussion

In this study we identified a new neuronal role for the mitogen-activated protein kinase kinase SEK-1 and the p38 MAPK pathway as a positive regulator of locomotion

and Gq signaling. The p38 MAPK pathway has been best characterized as a pathway activated by a variety of cellular stresses and inflammatory cytokines (Kyriakis and Avruch, 2012), but it has also been implicated in neuronal function, including some forms of mammalian synaptic plasticity (Bolshakov *et al.* 2000; Rush *et al.* 2002; Huang *et al.* 2004). In *C. elegans*, Gq plays a positive role in locomotion by promoting acetylcholine release, so we tested whether the slow locomotion of *sek-1* mutants is directly related to the role of *sek-1* as a regulator of Gq signaling. Through rescue experiments, we found that SEK-1 acts in acetylcholine neurons to regulate both the rate of locomotion and Gq signaling. Previously, *sek-1* has been shown to act in GABA neurons to regulate sensitivity to the acetylcholinesterase inhibitor aldicarb (Vashlishan et al., 2008), and to act in interneurons to regulate trafficking of the GLR-1 glutamate receptor and the frequency of worm reversals (Park and Rongo, 2016). Thus, *sek-1* may play distinct roles in different neuron types. Our data indicate a role for *sek-1* as a positive regulator of Gq signaling in acetylcholine neurons.

In addition to SEK-1, we identified other p38 pathway components regulating Gq signaling. Specifically, we found that mutants in *tir-1*, *nsy-1* and a *pmk-1 pmk-2* double mutant exhibit locomotion defects identical to *sek-1* and suppress activated Gq, suggesting that they act in a single p38 pathway to modulate signaling downstream of Gq. These results indicate a redundant function for PMK-1 and PMK-2 in regulating locomotion rate and Gq signaling. PMK-1 and PMK-2 also act redundantly for development of the asymmetric AWC neurons and to regulate induction of serotonin biosynthesis in the ADF neurons in response to pathogenic bacteria (Pagano et al.,

403 2015). By contrast, PMK-1 acts alone in the intestine to regulate innate immunity and in
404 interneurons to regulate GLR-1 trafficking (Pagano et al., 2015; Park and Rongo, 2016).
405 What is the downstream effector of *sek-1* p38 MAPK signaling in this Gq
406 signaling pathway? There are several known downstream effectors of p38 MAPK
407 signaling in *C. elegans*, including the transcription factor ATF-7 (Shivers et al., 2010;
408 Inoue et al., 2005; Xie et al., 2013). Our data indicate that ATF-7 is not required for the
409 p38 MAPK-dependent regulation of Gq signaling. It is possible that this p38 MAPK
410 pathway activates molecules other than transcription factors to regulate Gq signaling. It
411 is also possible that the *sek-1* p38 pathway activates multiple downstream effectors that
412 are not individually required.
413 One of the pathways that transduce signals from Gq includes the RhoGEF
414 Trio/UNC-73, the small GTPase Rho, and the cation channel NALCN/NCA-1 (Williams
415 et al., 2007; Topalidou et al., 2016b). We found that mutations in the *sek-1* p38 MAPK
416 pathway partially suppress an activated NCA-1 mutant and that *sek-1* probably acts to
417 control NCA-1 activity in the same neurons where it acts to regulate locomotion and Gq
418 signaling. Given the precedence for direct phosphorylation of sodium channels by p38
419 to regulate channel properties (Wittmack et al., 2005; Hudmon et al., 2008), it is
420 possible that PMK-1 and PMK-2 phosphorylate NCA-1 to regulate its expression,
421 localization, or activity. Our genetic study sets the foundation for further investigation of
422 the specific role of the *sek-1* p38 pathway in the regulation of Gq signaling and NCA-1
423 channel activity.
424
425 **Acknowledgements**

We thank Dennis Kim and Chiou-Fen Chuang for strains, Pin-An Chen and Erik Jorgensen for the *nca-1(gf)* mutant *ox352*, Chris Johnson for the fine mapping of *yak42*, Jordan Hoyt for help with Galaxy and CloudMap to analyze WGS data, and Dana Miller for providing access to her microscope camera. Some strains were provided by the CGC, which is funded by NIH Office of Research Infrastructure Programs (P40 OD010440). J.M.H was supported in part by Public Health Service, National Research Service Award T32GM007270, from the National Institute of General Medical Sciences. M.A. is an Ellison Medical Foundation New Scholar. This work was supported by NIH grant R00 MH082109 to M.A.

Figure Legends

Figure 1: *sek-1* acts downstream of Gαq to regulate locomotion behavior

(a) Gene structure of *sek-1*. White boxes depict the 5' and 3' untranslated regions, black boxes depict exons, and lines show introns. The positions of the *yak42* and *km4* deletions are shown. *yak42* is a 3713 bp deletion that extends to 1926 bp upstream of the start codon. Drawn with Exon-Intron Graphic Maker (http://www.wormweb.org/exonintron). Scale bar is 100 bp.

(b) *sek-1(yak42)* and *sek-1(km4)* suppress the small size and loopy waveform of *egl-30(tg26)*, written here as *egl-30(gf). unc-82(e1220)* does not suppress *egl-30(gf).* Photos of first-day adult worms. WT: wild type.

(c) *egl-30(gf)* is hyperactive compared to wild-type and suppressed by *sek-1(yak42)* and *sek-1(km4)*. ***, $p<0.001$, error bars = SEM, n=20.

448 (d) *sek-1* mutant worms have slow locomotion. ***, p<0.001 compared to wild-type, error
449 bars = SEM, n=20.
450
451 **Figure 2: *sek-1* acts in mature acetylcholine neurons to regulate locomotion**
452 (A) *sek-1* acts in neurons to regulate locomotion. The *sek-1* wild-type cDNA driven by
453 the *unc-119* pan-neuronal promoter *[unc-119p::sek-1(+)]* rescues the slow locomotion
454 phenotype of *sek-1(km4)* worms. ***, p< 0.001, error bars = SEM, n=20.
455 (B) *sek-1* acts in acetylcholine neurons to regulate locomotion. *sek-1* WT cDNA driven
456 by the *unc-17* acetylcholine neuron promoter *[unc-17p::sek-1(+)]* rescues the slow
457 locomotion phenotype of *sek-1(km4)* worms but *sek-1* expression in GABA neurons
458 using the *unc-47* promoter *[unc-47p::sek-1(+)]* does not. p< 0.001, error bars = SEM,
459 n=20.
460 (C-D) *sek-1* acts in acetylcholine neurons to suppress *egl-30(gf).* Worms expressing
461 *unc-119p::sek-1(+)* or *unc-17p::sek-1(+)* do not have the *egl-30(gf) sek-1* phenotype but
462 worms expressing *unc-47p::sek-1(+)* are identical to *egl-30(gf) sek-1* both for waveform
463 (C) and in the locomotion assay (D). Kruskal-Wallis test, ***, p< 0.001, **, p<0.01; error
464 bars = SEM, n=17-20.
465 (E) *sek-1* acts in mature neurons to regulate locomotion. *hsp-16.2p::sek-1(+)* rescues
466 the slow locomotion phenotype of *sek-1(km4)*. ***, p< 0.001, error bars = SEM, n=20.
467
468 **Figure 3: The p38 MAPK pathway regulates locomotion downstream of *egl-30***
469 (A) *tir-1(tm3036)* mutant animals have slow locomotion. ***, p<0.001, error bars = SEM,
470 n=20.

(B) *tir-1(tm3036)* suppresses *egl-30(gf)*. *egl-30(gf) tir-1* animals move more slowly than the hyperactive *egl-30(gf)* animals. ***, p< 0.001, error bars = SEM, n=20.

(C) *nsy-1(ok593)* mutant animals have slow locomotion. ***, p<0.001, error bars = SEM, n=20.

(D) *nsy-1(ok593)* suppresses *egl-30(gf)*. *egl-30(gf) nsy-1* animals move more slowly than the hyperactive *egl-30(gf)* animals. ***, p< 0.001, error bars = SEM, n=20.

(E) *pmk-2, pmk-2 pmk-1,* and *pmk-3* mutant animals have slow locomotion. ***, p< 0.001; *, p<0.05, compared to WT, error bars = SEM, n=20.

(F) A *pmk-2 pmk-1* double mutant suppresses the hyperactivity of *egl-30(gf)*. ***, p< 0.001, error bars = SEM, n=20.

(G) A *pmk-2 pmk-1* double mutant suppresses the deep body bends of *egl-30(gf)*. *egl-30(gf)* animals with mutations in either *pmk-1, pmk-2,* or *pmk-3* are still small and loopy. *egl-30(gf) pmk-2 pmk-1* animals are less loopy and have a more wild-type posture.

Figure 4: *sek-1* acts in the same genetic pathway as *unc-73*

(A) *sek-1* does not act in the same genetic pathway as *egl-8.* The *sek-1(km4)* mutation enhances the slow locomotion of *egl-8(sa47)* mutants. ***, p< 0.001, error bars = SEM, n=20.

(B) *sek-1* does not act in the same genetic pathway as *rund-1*. The *sek-1(km4)* mutation enhances the slow locomotion of *rund-1(tm3622)* mutants. ***, p< 0.001, error bars = SEM, n=20.

(C) *sek-1* may act in the same genetic pathway as *unc-73*. The *sek-1(km4)* mutation does not enhance the slow locomotion phenotype of *unc-73* mutants. ns, p>0.05, error bars = SEM, n=20.

(D) *sek-1(km4)* does not suppress the high-amplitude waveform of *nzIs29 rho-1(gf)* animals. *rho-1(gf)* and *rho-1(gf) sek-1(km4)* animals have similar body posture.

(E) *sek-1(km4)* does not suppress the slow locomotion of *rho-1(gf)* animals. ***, p< 0.001, error bars = SEM, n=20.

Figure 5: *sek-1* and *nsy-1* weakly suppress *nca-1(gf)*

(a) *nca-1(gf)* mutants are small and tightly coiled. The phenotypes of these *nca-1(ox352)* animals are partially suppressed by *nsy-1(ok593)* and *sek-1(km4)*. Photos of first-day adults.

(b) *nsy-1* and *sek-1* suppress *nca-1(gf)* locomotion. *nca-1(gf)* animals travel a small distance from the center of the plate in the radial locomotion assay. *nca-1(gf) nsy-1(ok593)* and *nca-1(gf) sek-1(km4)* worms move further than *nca-1(gf)* worms. **, p<0.01; *, p<0.05. Error bars = SEM, n=30.

(c) Expression of *sek-1* in all neurons and in acetylcholine neurons partially reverts the *sek-1* mutant suppression of *nca-1(gf)* size and body posture. White arrowheads depict food piles created by *nca-1(gf) sek-1(km4)* animals due to their uncoordinated locomotion. Such food piles are not made by *nca-1(gf)* animals.

(d) None of the neuronal *sek-1* rescuing constructs revert the radial locomotion phenotype of *nca-1(gf) sek-1(km4)* animals. Although the pan-neuronal and acetylcholine neuron constructs revert the size phenotype of *nca-1(gf) sek-1(km4)*,

these animals do not move a significantly different distance than *nca-1(gf) sek-1(km4)* animals. ns, p>0.05. Error bars = SEM, n=19-24.

Figure S1: *sek-1* suppresses *egl-30(gf)* deep body bends

(a) *egl-30(gf)* mutants have deeper body bends than wild-type (WT) and *sek-1* mutations suppresses this loopy posture. Images show tracks of forward-moving first-day adults.

(b) Quantification of the waveform phenotype. ***, p<0.001, error bars = SEM, n=4-5.

(c) *sek-1(ag1)* mutant animals have slow locomotion. ***, p<0.001, error bars = SEM, n=10.

(d) *sek-1* suppresses *goa-1* hyperactivity. *goa-1(sa734) sek-1(km4)* animals move more slowly than *goa-1(sa734)* animals. ***, p<0.001, error bars = SEM, n=20.

Figure S2: Locomotion of p38 and JNK MAPK pathway mutants

(A) *tir-1(tm3036)* suppresses *egl-30(gf)*. *egl-30(gf) tir-1(tm3036)* animals are less loopy and have a more wild-type posture.

(B) *nsy-1(ok593)* suppresses *egl-30(gf)*. *egl-30(gf) nsy-1(ok593)* animals are less loopy and have a more wild-type posture.

(C) *jkk-1* and *jnk-1* act in parallel to *sek-1* and *pmk-2 pmk-1*. The *jnk-1(gk7) sek-1(km4)* double mutant and *pmk-2(qd279 qd171) pmk-1(km25) jkk-1(km2)* triple mutants move more slowly than the respective individual mutants. **, p< 0.01, *, p<0.05; error bars = SEM, n=20.

(D) Worms with gain-of-function or loss-of-function alleles of *atf-7* are slower than wild-type worms. p< 0.001, error bars = SEM, n=20.

(E) Worms lacking *gap-2* and *vhp-1* move like wild-type worms. Neither *gap-2(tm478)* nor *vhp-1(sa366)* confers a slow locomotion phenotype. ns, p>0.05 compared to WT, error bars = SEM, n=20.

(F-G) *tir-1(ky648gf)* animals do not have loopy or hyperactive locomotion. *tir-1(ky648gf)* worms have wild-type posture and are slower than wild-type animals. ***, p< 0.001, error bars = SEM, n=20.

Table S1: Strain List

Strain	Genotype
AU1	*sek-1(ag1)* X
BS3383	*pmk-3(ok169)* IV
CX3695	*kyIs140[str-2p::gfp, lin-15(+)]* I
CX5959	*kyIs140[str-2p::gfp, lin-15(+)]* I; *tir-1(ky648gf)* III
EG317	*unc-73(ox317)* I
EG1000	*dpy-5(e61)* I; *rol-6(e187)* II; *lon-1(e1820)* III
EG1020	*bli-6(sc16)* IV; *dpy-11(e224)* V; *lon-2(e678)* X
EG4782	*nzIs29[unc-17p::rho-1(G14V), unc-122::gfp]* II
EG5505	*rund-1(tm3622)* X
EG7989	*unc-119(ed3)* III; *oxTi668[eft-3p::TdTomato::H2B, Cb-unc-119(+)]* X
IG685	*tir-1(tm3036)* III
JN147	*gap-2(tm748)* X

JT47	*egl-8(sa47)* V
JT366	*vhp-1(sa366)* II
JT734	*goa-1(sa734)* I
KU2	*jkk-1(km2)* X
KU4	*sek-1(km4)* X
KU25	*pmk-1(km25)* IV
N2	Bristol wild isolate, standard lab wild-type
VC8	*jnk-1(gk7)* IV
VC390	*nsy-1(ok593)* IV
XZ42	*sek-1(yak42)* X
XZ1233	*egl-30(tg26)* I*; sek-1(yak42)* X
XZ1151	*egl-30(tg26)* I
XZ1566	*egl-8(sa47)* V*; sek-1(yak42)* X
XZ1567	*unc-73(ox317)* I*; sek-1(yak42)* X
XZ1574	*rund-1(tm3622) sek-1(yak42)* X
XZ1575	*egl-30(tg26)* I*; sek-1(km4)* X
XZ1588	*egl-30(tg26)* I*; nsy-1(ok593)* IV
XZ1589	*egl-30(tg26)* I*; sek-1(km4)* X*; qdEx8[unc-119p::sek-1::GFP, myo-2p::mStrawberry::unc-54-3'UTR]*
XZ1593	*egl-30(tg26)* I*; pmk-1(km25)* IV
XZ1642	*sek-1(km4)* X*; yakEx72[unc-17p::sek-1::tbb-2utr-operon-GFP::H2B::cye-1utr, myo-2p::mCherry]*
XZ1643	*sek-1(km4) X; yakEx73[unc-47p::sek-1::tbb-2utr-operon-GFP::H2B::cye-*

	1utr, myo-2p::mCherry]
XZ1717	*nzIs29[unc-17p::rho-1(G14V) unc-122::gfp]* II*; sek-1(km4)* X
XZ1770	*egl-30(tg26)* I*; pmk-2(qd279 qd171) pmk-1(km25)* IV
XZ1771	*egl-30(tg26)* I*; pmk-2(qd287)* IV
XZ1772	*egl-30(tg26)* I*; pmk-3(ok169)* IV
XZ1815	*egl-30(tg26)* I*; tir-1(tm3036)* III
XZ1816	*nca-1(ox352)* IV*; sek-1(km4)* X*; qdEx8[unc-119p::sek-1::GFP::unc-54-3' UTR, myo-2p::mStrawberry::unc-54-3'UTR]*
XZ1834	*egl-30(tg26)* I*; sek-1(km4)* X*; yakEx72[unc-17p::sek-1::tbb-2utr-operon-GFP::H2B::cye-1utr, myo-2p::mCherry]*
XZ1835	*nca-1(ox352)* IV*; sek-1(km4)* X*; yakEx72[unc-17p::sek-1::tbb-2utr-operon-GFP::H2B::cye-1utr, myo-2p::mCherry]*
XZ1861	*nca-1(ox352)* IV*; sek-1(km4)* X*; yakEx73[unc-47p::sek-1::tbb-2utr-operon-GFP::H2B::cye-1utr, myo-2p::mCherry]*
XZ1863	*egl-30(tg26)* I*; sek-1(km4)* X*; yakEx73[unc-47p::sek-1::tbb-2utr-operon-GFP::H2B::cye-1utr, myo-2p::mCherry]*
XZ1872	*jnk-1(gk7)* I*; sek-1(km4)* X
XZ1873	*pmk-2(qd279 qd171) pmk-1(km25)* IV*; jkk-1(km2)* X
XZ1937	*sek-1(km4)* X*; yakEx121[hsp-16.2p::sek-1::tbb-2-3' UTR::gld-1 operon linker::gfp::h2b, myo-2p::mCherry]*
XZ1939	*goa-1(sa734)* I*; sek-1(km4)* X
XZ1942	*tir-1(ky648gf)* III
ZD202	*sek-1(km4)* X*; qdEx8[unc-119p::sek-1::GFP::unc-54-3' UTR + myo-*

	2p::mStrawberry::unc-54-3'UTR]
ZD318	*agIs29 atf-7(qd22 qd130)* III
ZD442	*agIs29 atf-7(qd22)* III
ZD934	*pmk-2(qd279 qd171) pmk-1(km25)* IV
ZD1020	*pmk-2(qd287)* IV

547

548 **Table S2: Plasmids and Primers**

549 Gateway entry clones

Plasmid	Details
pJH21	*sek-1* cDNA [1-2]
pCFJ150	pDEST5605[4-3]
pCFJ326	*tbb-2utr-operon-GFP::H2B::cye-1utr* [2-3]
pMH522	*unc-47p* [4-1]
pGH1	*unc-17p* [4-1]
pCM1.56	*hsp-16.2p* [4-1]

550

551 Gateway Expression Constructs

Plasmid	Details	Used to make
pJH23	*unc-17p::sek-1:: tbb-2utr-operon-GFP::H2B::cye-1utr*	*yakEx72*
pJH24	*unc-47p::sek-1:: tbb-2utr-operon-GFP::H2B::cye-1utr*	*yakEx73*
pJH46	*hsp-16.2p::sek-1:: tbb-2utr-*	*yakEx121*

	operon-GFP::H2B::cye-1utr	

552

553 Primers

oJH114	GGGGACAAGTTTGTACAAAAAAGCAGGCTcaATGGAGCGAAAAGGACGTG	F to clone *sek-1* cDNA into [1-2]
oJH115	GGGGACCACTTTGTACAAGAAAGCTGGGTgTCATCGTCGCCAAACAGTG	R to clone *sek-1* cDNA into [1-2]

554

555

556 **Table S3: Statistical Tests**

Figure	Test	p value
1C	One-way ANOVA and Bonferroni's Multiple Comparison Test WT vs *egl-30(tg26)* (p<0.001) *egl-30(tg26)* vs *egl-30(tg26); sek-1(yak42)* (p<0.001) *egl-30(tg26)* vs *egl-30(tg26);sek-1(km4)* (p<0.001)	< 0.001
1D	One-way ANOVA and Dunnett's Multiple Comparison Test WT vs *sek-1(yak42)* (p<0.001) WT vs *sek-1(km4)* (p<0.001)	< 0.001

2A	One-way ANOVA and Bonferroni's Multiple Comparison Test *sek-1(km4)* vs *sek-1(km4); qdEx8[unc-119p::sek-1(+)]* (p<0.001)	< 0.001
2B	One-way ANOVA and Bonferroni's Multiple Comparison Test *sek-1(km4)* vs *sek-1(km4); yakEx72[unc-17p::sek-1(+)]* (p<0.001) *sek-1(km4)* vs *sek-1(km4); yakEx73[unc-47p::sek-1(+)]* (ns)	< 0.001
2D	Kruskal-Wallis Test and Dunn's Multiple Comparison Test *egl-30(tg26); sek-1(km4)* vs *egl-30(tg26); sek-1(km4); qdEx8[unc-119p::sek-1(+)]* (p<0.001) *egl-30(tg26); sek-1(km4)* vs *egl-30(tg26); sek-1(km4); yakEx72[unc-17p::sek-1(+)]* (p<0.01) *egl-30(tg26); sek-1(km4)* vs *egl-30(tg26); sek-1(km4); yakEx73[unc-47p::sek-1(+)]* (ns)	< 0.001
2E	One-way ANOVA and Bonferroni's Multiple Comparison Test *sek-1(km4)* vs *sek-1(km4); yakEx121[hsp-16.2p::sek-1(+)]* (p<0.001)	< 0.001
3A	Unpaired t test, two-tailed	< 0.001

3B	One-way ANOVA and Bonferroni's Multiple Comparison Test *egl-30(tg26)* vs *egl-30(tg26); tir-1(tm3036)* (p<0.001)	< 0.001
3C	Unpaired t test, two-tailed	< 0.001
3D	One-way ANOVA and Bonferroni's Multiple Comparison Test *egl-30(tg26)* vs *egl-30(tg26); nsy-1(ok593)* (p<0.001)	< 0.001
3E	One-way ANOVA and Dunnett's Multiple Comparison Test WT vs *pmk-1(km25)* (ns) WT vs *pmk-2(qd287)* (p<0.05) WT vs *pmk-2(qd279 qd171) pmk-1 (km25)* (p<0.001) WT vs *pmk-3(ok169)* (p<0.001)	< 0.001
3F	One-way ANOVA and Dunnett's Multiple Comparison Test *egl-30(tg26)* vs *egl-30(tg26); pmk-1(km25)* (p<0.001) *egl-30(tg26)* vs *egl-30(tg26); pmk-2(qd287)* (p<0.001) *egl-30(tg26)* vs *egl-30(tg26); pmk-2(qd279 qd171) pmk-1 (km25)* (p<0.001) *egl-30(tg26)* vs *egl-30(tg26); pmk-3(ok169)* (p<0.001)	< 0.001
4A	One-way ANOVA and Bonferroni's Multiple Comparison Test *egl-8(sa47)* vs *egl-8(sa47); sek-1(yak42)* (p<0.001)	< 0.001
4B	One-way ANOVA and Bonferroni's Multiple Comparison Test	< 0.001

	sek-1(yak42) vs *rund-1(tm3622); sek-1(yak42)* (p<0.001)	
4C	One-way ANOVA and Bonferroni's Multiple Comparison Test *unc-73(ox317)* vs *unc-73(ox317); sek-1(yak42)* (ns)	< 0.001
4E	One-way ANOVA and Bonferroni's Multiple Comparison Test *nzIs29[unc-17p::rho-1(G14V)]* vs *nzIs29[unc-17p::rho-1(G14V)]; sek-1(km4)* (p<0.001)	< 0.001
5B	One-way ANOVA and Bonferroni's Multiple Comparison Test WT vs *nca-1(ox352)* (p<0.001) *nca-1(ox352)* vs *nca-1(ox352); nsy-1(ok593)* (p<0.01) *nca-1(ox352)* vs *nca-1(ox352); sek-1(km4)* (p<0.05)	< 0.001
5D	Kruskal-Wallis Test and Dunn's Multiple Comparison Test *nca-1(ox352);sek-1(km4)* vs *nca-1(ox352);sek-1(km4); qdEx8[unc-119p::sek-1(+)]* (ns) *nca-1(ox352);sek-1(km4)* vs *nca-1(ox352);sek-1(km4); yakEx72[unc-17p::sek-1(+)]* (ns) *nca-1(ox352);sek-1(km4)* vs *nca-1(ox352);sek-1(km4); yakEx73[unc-47p::sek-1(+)]* (ns)	< 0.001
S1B	One-way ANOVA and Bonferroni's Multiple Comparison Test *egl-30(tg26)* vs *egl-30(tg26); sek-1(yak42)*	< 0.001

	(p<0.001) *egl-30(tg26)* vs *egl-30(tg26); sek-1(km4)* (p<0.001)	
S1C	One-way ANOVA and Newman-Keuls Multiple Comparison Test WT vs *sek-1(yak42)* (p<0.001) WT vs *sek-1(ag1)* (p<0.001) *sek-1(yak42)* vs *sek-1(ag1)* (ns)	< 0.001
S1D	One-way ANOVA and Bonferroni's Multiple Comparison Test WT vs *sek-1(km4)* (p<0.001) *goa-1(sa734)* vs *sek-1(km4)* (p<0.001) *goa-1(sa734); sek-1(km4)* vs *sek-1(km4)* (p<0.001)	< 0.001
S2C	One-way ANOVA and Bonferroni's Multiple Comparison Test *jnk-1(gk7)* vs *jnk-1(gk7); sek-1(km4)* (p<0.01) *jkk-1(km2) vs pmk-2(qd279 qd171) pmk-1 (km25); jkk-1(km2)* (p<0.05)	< 0.001
S2D	One-way ANOVA and Bonferroni's Multiple Comparison Test WT vs *atf-7(qd22)* (p<0.001) WT vs *atf-7(qd22 qd130)* (p<0.001)	< 0.001
S2E	One-way ANOVA	p=0.806

S2G	Unpaired t test, two-tailed	< 0.001

References

Ailion, M., M. Hannemann, S. Dalton, A. Pappas, S. Watanabe, *et al.,* 2014 Two Rab2 interactors regulate dense-core vesicle maturation. Neuron 82: 167–180.

Andrusiak, M. G., and Y. Jin, 2016 Context Specificity of Stress-activated Mitogen-activated Protein (MAP) Kinase Signaling: The Story as Told by *Caenorhabditis elegans*. J. Biol. Chem. 291: 7796–7804.

Bastiani, C. A., S. Gharib, M. I. Simon, and P. W. Sternberg, 2003 Caenorhabditis elegans Gαq Regulates Egg-Laying Behavior via a PLCβ-Independent and Serotonin-Dependent Signaling Pathway and Likely Functions Both in the Nervous System and in Muscle. Genetics 165: 1805–1822.

Bence, K., W. Ma, T. Kozasa, and X. -Y. Huang, 1997 Direct stimulation of Bruton's tyrosine kinase by Gq-protein α-subunit. Nature 389: 296–299.

Bolshakov V. Y., Carboni L., Cobb M. H., Siegelbaum S. A., Belardetti F., 2000 Dual MAP kinase pathways mediate opposing forms of long-term plasticity at CA3-CA1 synapses. Nat. Neurosci. **3**: 1107–1112.

Brenner, S., 1974 The genetics of Caenorhabditis elegans. Genetics 77: 71–94.

Chang, C., Y. -W. Hsieh, B. J. Lesch, C. I. Bargmann, and C. -F. Chuang, 2011 Microtubule-based localization of a synaptic calcium-signaling complex is required for left-right neuronal asymmetry in *C. elegans*. Development 138: 3509–3518.

577 Chuang, C. -F., and C. I. Bargmann, 2005 A Toll-interleukin 1 repeat protein at the
578 synapse specifies asymmetric odorant receptor expression via ASK1 MAPKKK
579 signaling. Genes Dev. 19: 270–281.

580 Couillault, C., N. Pujol, J. Reboul, L. Sabatier, J. -F. Guichou, *et al*., 2004 TLR-
581 independent control of innate immunity in Caenorhabditis elegans by the TIR domain
582 adaptor protein TIR-1, an ortholog of human SARM. Nat. Immunol. 5: 488–494.

583 Doi, M., and K. Iwasaki, 2002 Regulation of Retrograde Signaling at Neuromuscular
584 Junctions by the Novel C2 Domain Protein AEX-1. Neuron 33: 249–259.

585 Fay, D. 2006 Genetic mapping and manipulation: Chapter 7-Making compound
586 mutants. *WormBook*, ed. The *C. elegans* Research Community, WormBook,
587 doi/10.1895/wormbook.1.96.2, http://www.wormbook.org

588 Frøkjær-Jensen, C., M. W. Davis, M. Ailion, and E. M. Jorgensen 2012 Improved Mos1-
589 mediated transgenesis in *C. elegans*. Nat. Methods 9: 117–118.

590 Frokjaer-Jensen, C., M. W. Davis, M. Sarov, J. Taylor, S. Flibotte, *et al*., 2014 Random
591 and targeted transgene insertion in C. elegans using a modified Mosl transposon. Nat.
592 Methods 11: 529–534.

593 Gao, S., L. Xie, T. Kawano, M. D. Po, J. K. Pirri, *et al*., 2015 The NCA sodium leak
594 channel is required for persistent motor circuit activity that sustains locomotion. Nat.
595 Commun. 6: 6323.

García-Hoz, C., G. Sánchez-Fernández, M. T. Díaz-Mec, J. Moscat, F. Mayor *et al.*, 2010 Gαq Acts as an Adaptor Protein in Protein Kinase Cζ (PKCζ)-mediated ERK5 Activation by G Protein-coupled Receptors (GPCR). J. Biol. Chem. 285: 13480–13489.

Hajdu-Cronin, Y. M., W. J. Chen, G. Patikoglou, M. R. Koelle, and P. W. Sternberg, 1999 Antagonism between Goα and Gqα in Caenorhabditis elegans: the RGS protein EAT-16 is necessary for Goα signaling and regulates Gqα activity. Genes Dev. 13: 1780–1793.

Hoppe, P. E., J. Chau, K. A. Flanagan, A. R. Reedy, and L. A. Schriefer, 2010 *Caenorhabditis elegans unc-82* Encodes a Serine/Threonine Kinase Important for Myosin Filament Organization in Muscle During Growth. Genetics 184: 79–90.

Huang, C. -C., J. -L. You, M. -Y. Wu, and K. -S. Hsu, 2004 Rap1-induced p38 mitogen-activated protein kinase activation facilitates AMPA receptor trafficking via the GDI.Rab5 complex. Potential role in (S)-3,5-dihydroxyphenylglycene-induced long term depression. J. Biol. Chem. 279: 12286–12292.

Hudmon, A., J. -S. Choi, L. Tyrrell, J. A. Black, A. M. Rush, *et al*., 2008 Phosphorylation of Sodium Channel Nav1.8 by p38 Mitogen-Activated Protein Kinase Increases Current Density in Dorsal Root Ganglion Neurons. J. Neurosci. 28: 3190–3201.

Inoue, H., N. Hisamoto, J. H. An, R. P. Oliveira, E. Nishida, *et al*., 2005 The *C. elegans* p38 MAPK pathway regulates nuclear localization of the transcription factor SKN-1 in oxidative stress response. Genes Dev. 19: 2278–2283.

616 Jantsch-Plunger, V., P. Gönczy, A. Romano, H. Schnabel, D. Hamill, *et al.*, 2000 CYK-
617 4: A Rho family gtpase activating protein (GAP) required for central spindle formation
618 and cytokinesis. J. Cell Biol. 149: 1391–1404.

619 Kawasaki, M., N. Hisamoto, Y. Iino, M. Yamamoto, J. Ninomiya-Tsuji , *et al.*, 1999 A
620 *Caenorhabditis elegans* JNK signal transduction pathway regulates coordinated
621 movement via type-D GABAergic motor neurons. EMBO J. 18: 3604–3615.

622 Kim, D.H., R. Feinbaum, G. Alloing, F. E. Emerson, D. A. Garsin, *et al.*, 2002 A
623 Conserved p38 MAP Kinase Pathway in *Caenorhabditis elegans* Innate Immunity.
624 Science 297: 623–626.

625 Kim, D.H., N. T. Liberati, T. Mizuno, H. Inoue, N. Hisamoto, *et al.*, 2004 Integration of
626 *Caenorhabditis elegans* MAPK pathways mediating immunity and stress resistance by
627 MEK-1 MAPK kinase and VHP-1 MAPK phosphatase. Proc. Natl. Acad. Sci. U. S. A.
628 101: 10990–10994.

629 Koelle, M. R., 2016 Neurotransmitter signaling through heterotrimeric G proteins:
630 insights from studies in *C. elegans*. WormBook, doi:10.1895/wormbook.1.75.2.

631 Kyriakis, J. M., and J. Avruch, 2012 Mammalian MAPK signal transduction pathways
632 activated by stress and inflammation: a 10-year update. Physiol. Rev. 92:689-737.

633 Lackner, M. R., S. J. Nurrish, and J. M. Kaplan, 1999 Facilitation of Synaptic
634 Transmission by EGL-30 Gqα and EGL-8 PLCβ: DAG Binding to UNC-13 Is Required to
635 Stimulate Acetylcholine Release. Neuron 24: 335–346.

636 Lu, B., Y. Su, S. Das, J. Liu, J. Xia, *et al*., 2007 The Neuronal Channel NALCN
637 Contributes Resting Sodium Permeability and Is Required for Normal Respiratory
638 Rhythm. Cell 129: 371–383.

639 McMullan, R., E. Hiley, P. Morrison, and S. J. Nurrish 2006 Rho is a presynaptic
640 activator of neurotransmitter release at pre-existing synapses in *C. elegans*. Genes
641 Dev. 20: 65–76.

642 Mello, C. C., J. M. Kramer, D. Stinchcomb, and V. Ambros, 1991 Efficient gene transfer
643 in C.elegans: extrachromosomal maintenance and integration of transforming
644 sequences. EMBO J. 10: 3959–3970.

645 Miller, K. G., M. D. Emerson, and J. B. Rand 1999 Goα and Diacylglycerol Kinase
646 Negatively Regulate the Gqα Pathway in *C. elegans*. Neuron 24: 323–333.

647 Minevich, G., D. S. Park, D. Blankenberg, R. J. Poole, and O. Hobert, 2012 CloudMap:
648 a cloud-based pipeline for analysis of mutant genome sequences. Genetics 192: 1249–
649 1269.

650 Nash, H. A., R. L. Scott, B. C. Lear, and R. Allada, 2002 An unusual cation channel
651 mediates photic control of locomotion in *Drosophila*. Curr. Biol. 12: 2152–2158.

652 Nurrish S., Ségalat L., Kaplan J. M., 1999 Serotonin inhibition of synaptic transmission:
653 Galpha(0) decreases the abundance of UNC-13 at release sites. Neuron 24: 231–242.

654 Pagano, D. J., E. R. Kingston, and D. H. Kim, 2015 Tissue Expression Pattern of PMK-2
655 p38 MAPK Is Established by the miR-58 Family in *C. elegans*. PLOS Genet 11:
656 e1004997.

657 Park, E.C., and Rongo, C. (2016). The p38 MAP kinase pathway modulates the hypoxia
658 response and glutamate receptor trafficking in aging neurons. eLife *5*, e12010.

659 Plowman, G. D., S. Sudarsanam, J. Bingham, D. Whyte, and T. Hunter, 1999 The
660 protein kinases of *Caenorhabditis elegans*: a model for signal transduction in
661 multicellular organisms. Proc. Natl. Acad. Sci. U. S. A. 96: 13603–13610.

662 Rhee, S. G. 2001 Regulation of Phosphoinositide-Specific Phospholipase C. Annu. Rev.
663 Biochem. 70: 281–312.

664 Rush A. M., Wu J., Rowan M. J., Anwyl R., 2002 Group I metabotropic glutamate
665 receptor (mGluR)-dependent long-term depression mediated via p38 mitogen-activated
666 protein kinase is inhibited by previous high-frequency stimulation and activation of
667 mGluRs and protein kinase C in the rat dentate gyrus in vitro. J. Neurosci. 22: 6121–
668 6128.

669 Sagasti, A., N. Hisamoto, J. Hyodo, M. Tanaka-Hino, K. Matsumoto, *et al.*, (2001). The
670 CaMKII UNC-43 Activates the MAPKKK NSY-1 to Execute a Lateral Signaling Decision
671 Required for Asymmetric Olfactory Neuron Fates. Cell 105: 221–232.

672 Sánchez-Fernández, G., S. Cabezudo, C. García-Hoz, C. Benincá, A. M. Aragay, *et al.*,
673 (2014). Gαq signalling: The new and the old. Cell. Signal. 26: 833–848.

674 Shi, Y., C. Abe, B. B. Holloway, S. Shu, N. N. Kumar, *et al.*, 2016 Nalcn Is a “Leak”
675 Sodium Channel That Regulates Excitability of Brainstem Chemosensory Neurons and
676 Breathing. J. Neurosci. 36: 8174–8187.

677 Shivers, R. P., D. J. Pagano, T. Kooistra, C. E. Richardson, K. C. Reddy, *et al*., 2010
678 Phosphorylation of the conserved transcription factor ATF-7 by PMK-1 p38 MAPK
679 regulates innate immunity in *Caenorhabditis elegans*. PLoS Genet. 6: e1000892.

680 Tanaka-Hino, M., A. Sagasti, N. Hisamoto, M. Kawasaki, S. Nakano, *et al*., 2002 SEK-1
681 MAPKK mediates Ca2+ signaling to determine neuronal asymmetric development in
682 *Caenorhabditis elegans*. EMBO Rep. 3: 56–62.

683 Topalidou, I., J. Cattin-Ortolá, A. L. Pappas, K. Cooper, G. E. Merrihew, *et al*., 2016a
684 The EARP Complex and Its Interactor EIPR-1 Are Required for Cargo Sorting to Dense-
685 Core Vesicles. PLOS Genet 12: e1006074.

686 Topalidou I., Chen P.-A., Cooper K., Watanabe S., Jorgensen E. M., *et al*.., 2016b The
687 NCA-1 ion channel functions downstream of Gq and Rho to regulate locomotion in C.
688 elegans. bioRxiv. doi: http://dx.doi.org/10.1101/090514

689 Vaqué, J. P., R. T. Dorsam, X. Feng, R. Iglesias-Bartolome, D. J. Forsthoefel, *et al.*,
690 2013 A genome-wide RNAi screen reveals a Trio-regulated Rho GTPase circuitry
691 transducing mitogenic signals initiated by G protein-coupled receptors. Mol. Cell 49: 94–
692 108.

693 Vashlishan, A. B., J. M. Madison, M. Dybbs, M., J. Bai, D. Sieburth, *et al.*, 2008 An
694 RNAi Screen Identifies Genes that Regulate GABA Synapses. Neuron 58: 346–361.

695 Williams, S. L., S. Lutz, N. K. Charlie, C. Vettel, M. Ailion, *et al.*, 2007 Trio's Rho-
696 specific GEF domain is the missing Galpha q effector in *C. elegans*. Genes Dev. 21:
697 2731–2746.

698 Wittmack, E. K., A. M. Rush, A. Hudmon, S. G. Waxman, and S. D. Dib-Hajj, 2005
699 Voltage-Gated Sodium Channel Nav1.6 Is Modulated by p38 Mitogen-Activated Protein
700 Kinase. J. Neurosci. 25: 6621–6630.

701 Xie, Y., M. Moussaif, S. Choi, L. Xu, and J. Y. Sze, 2013 RFX transcription factor DAF-
702 19 regulates 5-HT and innate immune responses to pathogenic bacteria in
703 *Caenorhabditis elegans*. PLoS Genet. 9: e1003324.

704 Zhang, R., X. He, W. Liu, M. Lu, J. -T. Hsieh, *et al.*, 2003 AIP1 mediates TNF-α–
705 induced ASK1 activation by facilitating dissociation of ASK1 from its inhibitor 14-3-3. J.
706 Clin. Invest. 111: 1933–1943.

707

Figure 1

A

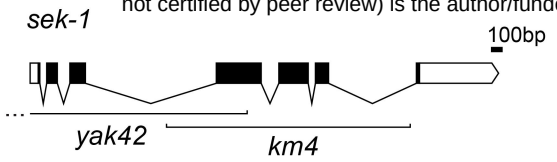

B

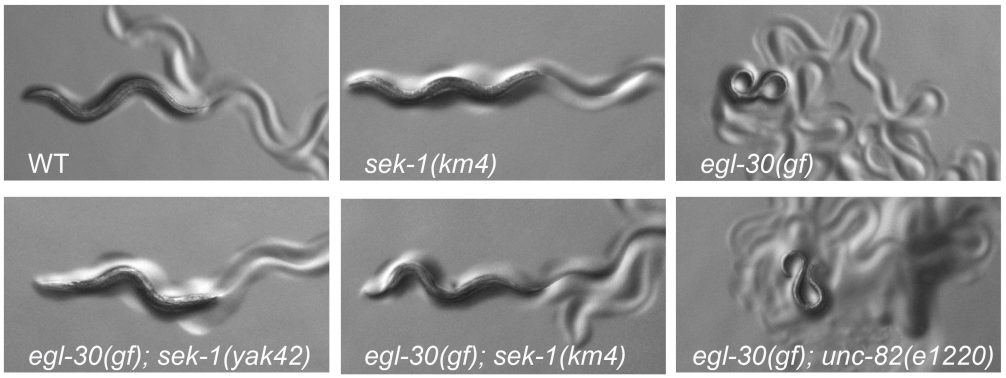

C

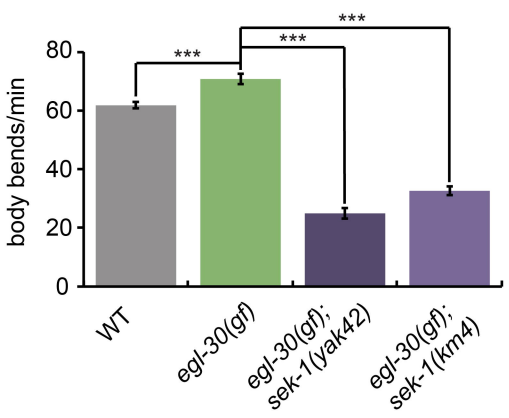

D

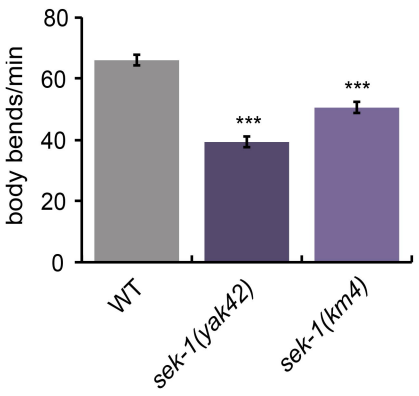

Figure 2

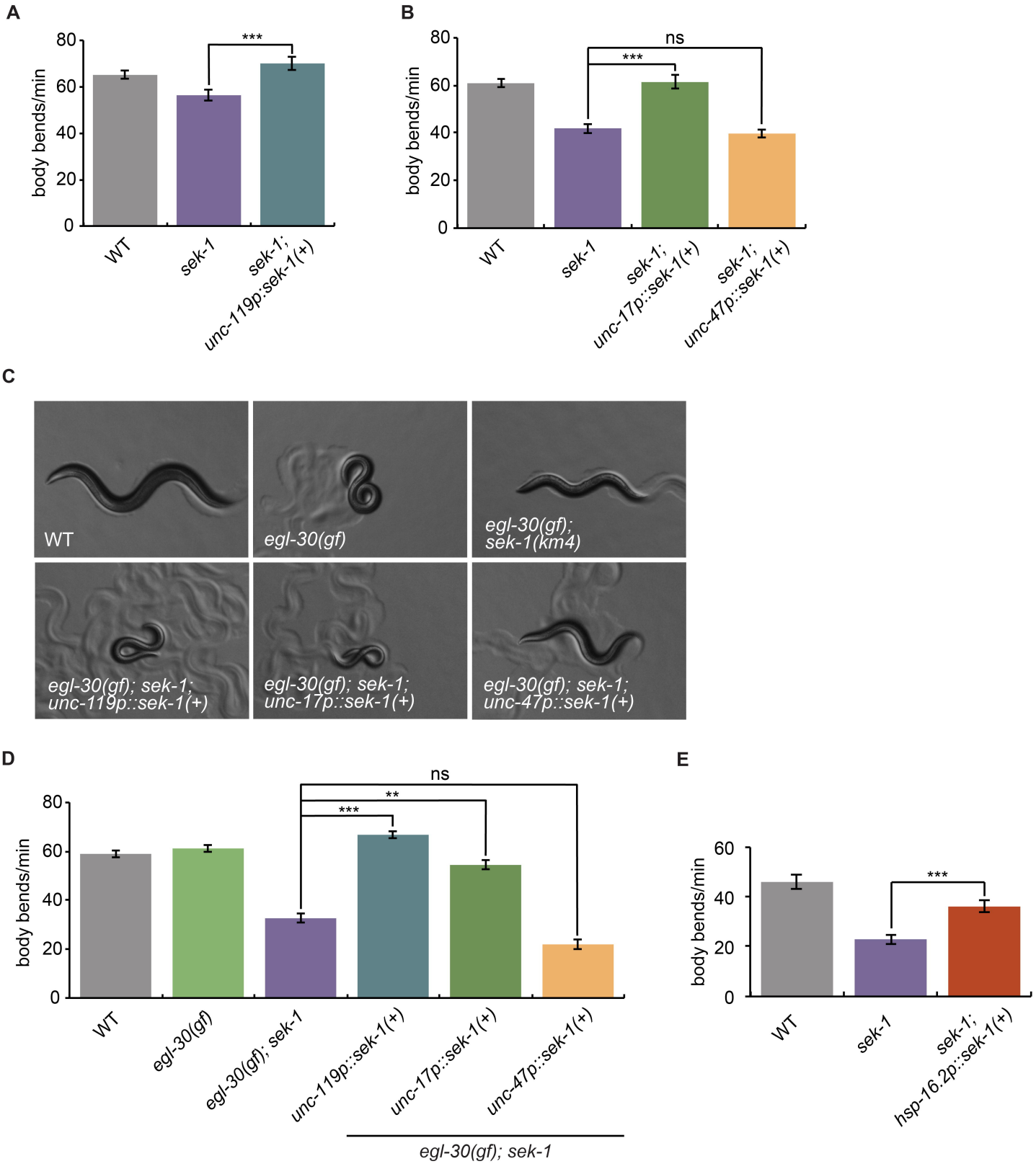

Figure 3

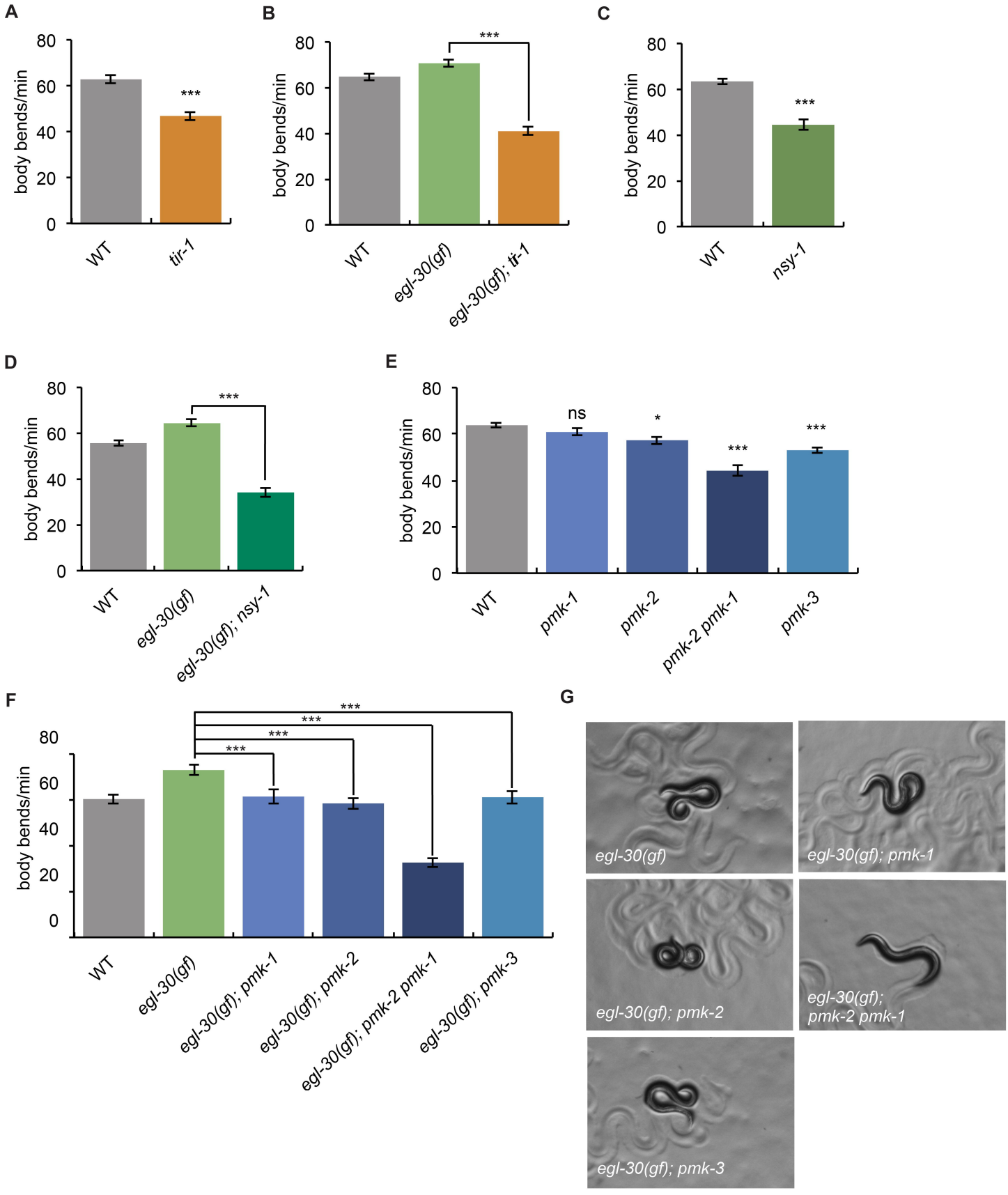

Figure 4

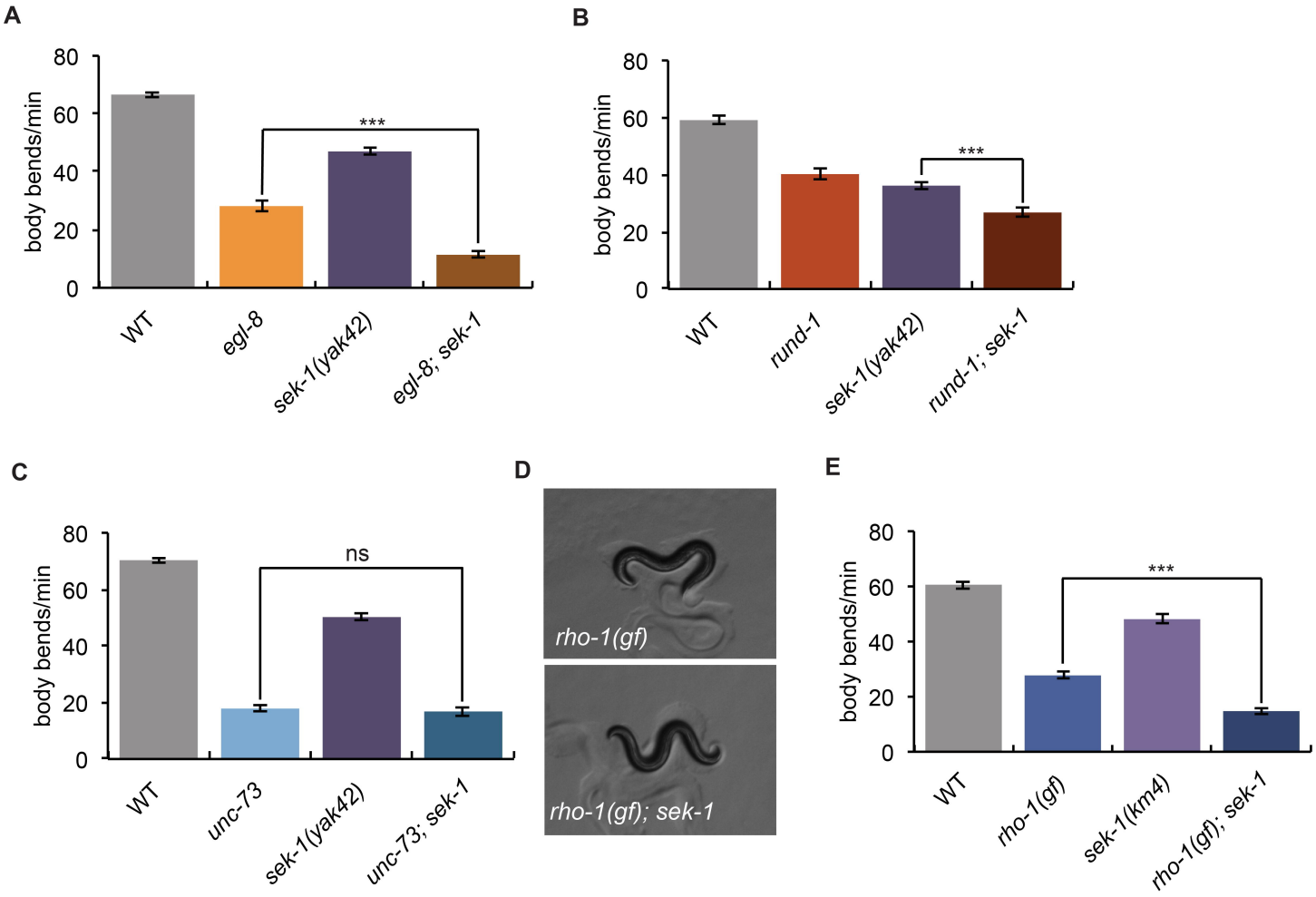

Figure 5